NANO LETTERS

2007
Vol. 7, No. 1
64−68

Tip Cooling Effect and Failure Mechanism of Field-Emitting Carbon Nanotubes

Wei Wei,[†] Yang Liu,[‡] Yang Wei,[†] Kaili Jiang,*[,†] Lian-Mao Peng,*[,‡] and Shoushan Fan*[,†]

Department of Physics and Tsinghua-Foxconn Nanotechnology Research Center, Tsinghua University, Beijing 100084, China, and Key Laboratory for the Physics and Chemistry of Nanodevices and Department of Electronics, Peking University, Beijing 100871, China

Received August 23, 2006; Revised Manuscript Received October 31, 2006

ABSTRACT

The cooling effect accompanying field electron emission has been considered for a single carbon nanotube (CNT) used as a field emission (FE) electron source. An improved model for the failure mechanism of field emitting CNTs has been proposed and validated. Our model predicts a maximum temperature (T-max) located at an interior point rather than the tip of the CNTs, and the failure of the CNT emitters tends to take place at the T-max point, inducing a segment by segment breakdown process. A combination of Joule heating and electrostatic force effect is proposed responsible for initiating the failure of the field emitting CNT and validated by in situ FE observation.

Carbon nanotubes (CNTs) are promising field emission electron sources with advantages of high brightness, high monochromaticity, and low power consumption,[1] which can be applied in various devices such as flat panel displays,[2] electron guns,[3,4] X-ray sources,[5] etc. The field emitting materials, however, are requested to withstand the high-temperature caused by Joule heating and the high tensile stress exerted by the electric field (E-field) to avoid device failure.[1] In the case of CNTs, both the high temperature[6] and tensile stress[7] have been measured during FE. Device failures due to both effects have been intensely investigated.[6,8−13] Concerning the temperature effect, Vincent et al. have proposed a model to calculate the temperature distribution along CNTs during FE,[8] which predicts a maximum temperature at the CNT's tip. Later, this model was slightly modified by Huang et al., which predicts that the tip temperature will go to infinity when the emission current is above a critical value.[9] If the maximum temperature is located at CNT's tip, a gradual shortening is expected to occur at the tip of the CNT when it reaches the critical current. In many cases, however, the CNTs are shortened segment by segment, rather than shortened gradually, according to in situ transmission electron microscopy (TEM) observations by Wang et al.[10] and Doytcheva et al.[13] To solve this puzzle, we conducted both theoretical modeling and a series of experiments. We found that this phenomenon can be well interpreted by considering the heat taken away by emission electrons, which was further verified by our experimental results. On the basis of this model, the failure mechanisms of the CNT emitters were proposed and validated.

More than 100 years ago, Richardson theoretically predicted the cooling effect in thermionic emission;[14] that is, the evaporation of electrons from the surface of a hot conductor is very similar to the evaporation of molecules from a liquid, causing a cooling of the surface.[15] In his paper,[14] Richardson argued that the cooling effect induced by electron emission is less prominent than that by thermal radiation for metals at less than 2000 K, but in the case of carbon, the cooling effect became prominent at temperatures above 2000 °C. As is well-known, FE is a quantum tunneling process, implying no energy loss when electrons pass through the cathode−vacuum barrier. When an electron is field emitted from a cathode at temperature T, it will take away an energy of about $(3/2)k_BT$, inducing a cooling effect. For FE from CNTs, Vincent et al. have measured a tip temperature of about 2000 K at an emission current of 2 μA.[8] On the basis of their data, a rough estimation indicates that the energy loss due to electron emission is more than 4600 times that due to thermal radiation, which shows the cooling effect in FE is much more prominent than that in thermionic

* Corresponding authors. E-mail: jiangkl@tsinghua.edu.cn, lmpeng@pku.edu.cn, and fss-dmp@tsinghua.edu.cn.

[†] Department of Physics and Tsinghua-Foxconn Nanotechnology Research Center, Tsinghua University.

[‡] Key Laboratory for the Physics and Chemistry of Nanodevices and Department of Electronics, Peking University.

10.1021/nl061982u CCC: $37.00 © 2007 American Chemical Society
Published on Web 12/01/2006

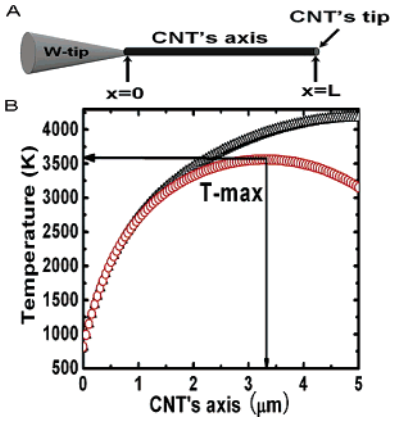

Figure 1. (A) Illustration of our modeled field emission cathode. (B) The comparison of the temperature distributions along the CNT's axis with (red circles) or without (black triangles) considering the heat loss accompanying electron emission. The CNT here was assumed to be 5 μm in length and 10 nm in diameter, and the emission current was 10 μA.

emission. The reason lies in the fact that the CNT emitter has an extraordinarily large emission current density (10^6 A/cm^2) from an extremely small emitting area (10^{-12} cm^2). Therefore, the cooling effect due to electron emission must be taken into consideration when calculating the temperature distribution along CNTs during FE.

Following refs 8 and 9, we calculated the temperature distribution along the axis direction (x-axis) of a field-emitting CNT by modeling it as a one-dimensional object of length L in contact with a microtip substrate (W-tip in our experiment). There is a stable Joule heating $dQ = I^2\rho(T_x)dx/(\pi r^2)$ during the FE process (Figure 1A), where I is the emission current, T_x the temperature at x point, r the radius of CNTs, and ρ the resistivity of CNTs which is temperature-dependent due to different conduction mechanisms and assumed the same expression as in ref 9

$$\rho(T_x) = \rho_0(1 - \alpha T_x + \beta T_x^{3/2})$$

where ρ_0 is the resistivity of the CNT at room temperature, which was measured by a two-probe configuration (2P) in our experiment.[16] The time-independent heat equation during FE is

$$\pi r^2 \kappa \frac{\partial^2 T_x}{\partial x^2} \mathrm{d}x - 2\pi r \,\mathrm{d}x\, \sigma(T_x^4 - T_0^4) + \frac{I^2\rho(T_x)}{\pi r^2}\mathrm{d}x = 0 \quad (1)$$

where σ is the Stefan−Boltzmann constant (we assume emissivity = 1), κ is the thermal conductivity, and T_0 is the ambient temperature (300 K).

Heat loss to the microtip can be determined by an empirical expression[9]

$$T_{x=0} = \lambda\pi r^2 \kappa \left.\frac{\partial T_x}{\partial x}\right|_{x=0} + T_0 \quad (2)$$

where λ is a constant, determined by the contact resistance and the shape of the microtip, and can be chosen to match the experimental data.

Since the cooling effect accompanying electron emission is prominent, the term of the heat loss due to the electron emission has to be taken into consideration in the boundary condition at the CNT's tip. Assuming the energy of one emission electron is $E_0 = (3/2)k_B T_{x=L}$ where k_B is Boltzmann constant and $T_{x=L}$ the temperature of the emitter's apex (i.e., tip temperature T_A), heat loss due to electron emission and radiation from the tip can be determined by

$$\left.\frac{\partial T_x}{\partial x}\right|_{x=L} = -\sigma\kappa^{-1}(T_{x=L}^4 - T_0^4) - \frac{3}{2}\kappa^{-1}\frac{k_B T_{x=L} I}{e\pi r^2} \quad (3)$$

With the boundary conditions of eqs 2 and 3 and experiment parameters,[16] by solving eq 1, the temperature distribution T_x along the CNT's axis can be obtained.

In Figure 1B, black triangles represent the calculated temperature distribution based on the model of Vincent et al.[8] and Huang et al.[9] Red circles are the result of our model including the cooling effect accompanying electron emission. The T-max has a 600 K difference between the predictions of these two models, indicating the cooling effect is obvious in FE. Furthermore, our model predicts that T-max point is located at an interior point rather than the CNT's tip, which is 410 K higher than T_A. The models of Vincent et al.[8] and Huang et al.[9] predict that the failure due to temperature effects occurs at the CNT's tip. In contrast, our model predicts that the failure occurs at an interior point near the tip owing to the location of the T-max point, indicating the CNT will be shortened segment by segment.

To validate our model, an individual field emitting CNT was investigated in situ in a 200 keV Tecnai G20 transmission electron microscope (TEM) with a vacuum about 10^{-8} Torr. An individual CNT was mounted on a W-tip of a scanning tunneling microscope (Nanofactory) inside the TEM to serve as a cathode. A bias was applied between the CNT and counter Pt electrode for in situ FE investigation. Experimental details can be found in Supporting Information.[16]

According to previous investigations, the failure of field emitters can be summarized as a consequence of two effects, the force effect (F-effect) and the temperature effect (T-effect). The former originates from the Maxwell stress exerted by the E-field on the surface of a conductor, which can be further divided into axial stress and radial stress in the case of field emitting CNTs. The axial stress will break or tear away the CNT,[7,11] while the radial stress might cause the CNT's tip splitting.[10,13] The latter due to the Joule heating at large current might lead to wall-by-wall breakdown of CNTs.[17,18]

In the case of a CNT attached on a microtip, failure occurs most frequently at the weak contact between the CNT and the microtip; that is, the CNT may be wholly removed from the microtip when the current density is not very high.[11] This failure regime is largely attributed to the F-effect. To ensure a good contact, both electrical and mechanical, we therefore deposited amorphous carbon on the contact via electron-

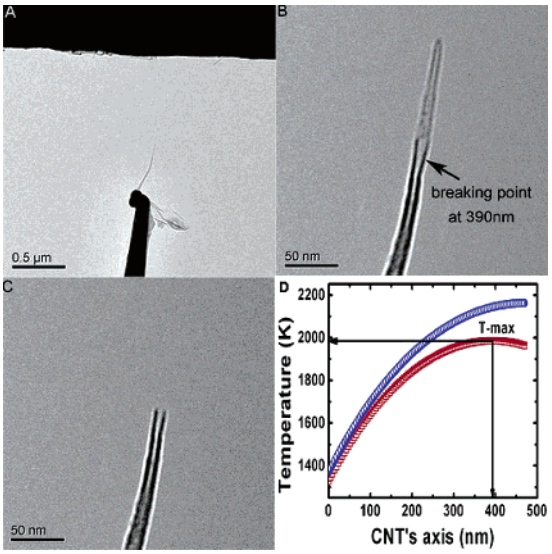

Figure 2. TEM images of the field emitting CNT before (A, B) and after (C) breakdown. (D) A comparison of temperature distributions along the CNT's axis given by the two models.

beam-induced deposition inside the TEM and then annealed the contact by a series of large current pulses.[16,19] The resulting robust contact enables us to investigate the FE from the individual CNT at large E-field and current density, as well as temperature-induced failure.

Parts A and B of Figure 2 show a 470 nm long CNT (sample1) fixed on a W-tip serving as cathode with a cathode−anode distance of 800 nm. At about 95 V (35 μA), the whole upper part of the CNT was removed abruptly with a current drop (Figure 2C). The breaking point at 390 nm of the CNT is very close to the T-max point at 394.8 nm predicted by our model (red plots of Figure 2D). The temperature distribution along the CNT without considering the cooling effect was also given for comparison (blue plots of Figure 2D) and the corresponding T-max point is at the apex of the CNT and about 177 K higher than our model.

Further analyzing the failure process, we gradually increased the bias during the FE measurement on sample 2 which is 330 nm in length and 14 nm in diameter with a cathode−anode distance of 600 nm (Figure 3A). Meanwhile, the images of the CNT during FE were recorded simultaneously. At the bias 88 V (40 μA), the left side of the graphite shell of the CNT at 280 nm began to cleave (Figure 3B,C), the cleft enlarged as the applied voltage was increased (Figure 3D), and the upper part of the CNT burned away gradually because the cleft slowed down the heat conduction (Figure 3E,F), and finally it was removed completely (Figure 3G). Through the same calculation as for sample1, the T-max point along the CNT for 88 V (40 μA) was at 283.8 nm, which is approximately equal to our experimental breaking point 280 nm.

We listed the results of our three samples and those of Doytcheva et al.[13] in Table 1. All the experimental breaking points are almost the same as the T-max points predicted by our model, indicating a strong correlation between the failure and the T-effect.

We could not, however, attribute the failure solely to the T-effect. As stated in Supporting Information,[16] our sample 1 was obtained by resistive heating a 1 μm long CNT which experienced wall-by-wall breakdown at a current of 81 μA. If only the T-effect was considered, the current capacity of sample1 should be at least 81 μA. Our sample 1, however, failed at a much smaller current 35 μA, indicating the failure was not only due to the T-effect but also to the F-effect of high E-field. The electrostatic force here can be estimated by integrating the stress over the outmost graphite shell of the nanotube as shown in ref 16. A breaking stress about 3.90 GPa in the outmost shell of sample 1 is much smaller than the tensile strength (11−63 GPa) for the outmost shell of the CNT,[20] indicating only the mechanical stress is also not large enough to destroy the CNT's graphite layer. The failures observed in our experiments are therefore due to a combination of T-effect and F-effect. The T-effect will lead to the evaporation of carbon atom in vacuum resulting in vacancy defects at high temperature (for our three samples, the calculated T-max at failure are all around 2000 K).[17,18] The F-effect will enlarge the defect forming a cleft at the T-max point. And then due to the increasing current density at this point, more heat will be released here inducing even higher temperature which makes the point thinner or the cleft larger, giving positive feedback to heating, and ultimately the segment above T-max point will be torn away by the E-field.

Figure 4A presents the calculated temperature distributions along the same CNT at a fixed emission current based on our model when its length varies. The reduction of the T-max is obvious when the length decreases. That is, when a CNT is shortened, its T-max decreases automatically. At the same time, the apparent E-field and field enhancement factor will also decrease, leading to the reduction of emission current and, consequently, the further reduction of T-max. Once the CNT is shortened, therefore, this negative feedback mechanism prevents the CNT from further degrading, and the CNT will stably emit electrons at a smaller current. To initiate next shortening of the CNT, increasing the bias is imperative according to our model and the experiments of Doytcheva et al.[13] and ours. Note that a similar negative feedback mechanism also exists in the models of Vincent et al.[8] and Huang et al.[9] (Figure 4B). But their models predict the T-max point is at the tip of the CNT. If the bias gradually increases, the CNT should be shortened gradually from the tip. However this is not observed by in situ TEM observations by Wang et al.,[10] Doytcheva et al.,[13] and us, in which the CNTs are shortened segment by segment from the T-max point as predicted by our model. In principle, if the CNT is open-ended with uniform diameter and the contact between the CNT and microtip is sufficiently strong, the CNT emitter will be shortened segment by segment until completely destroyed. In our experiment, however, this segment by segment breakdown mode usually interrupted by a total removal when the remaining CNT was very short (<300 nm). Compared with long CNTs, according to our calculations, the short CNT has much larger current capacity before its T-max point reaches 2000 K (Figure 4C). To initiate another

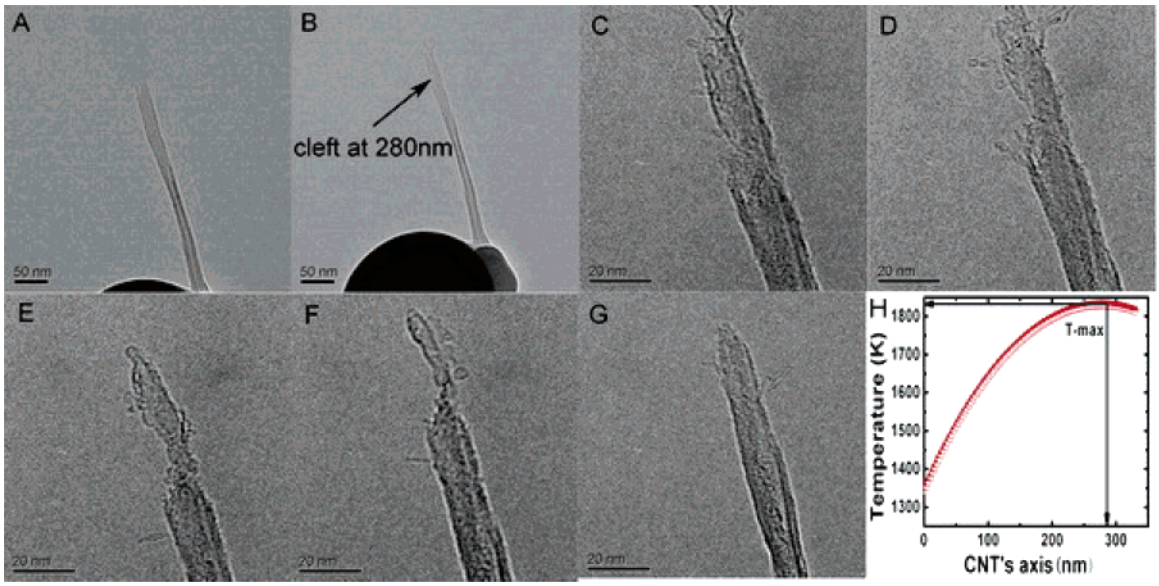

Figure 3. (A−G) The real-time TEM images showing the evolution of a CNT during FE and the failure process. (H) The corresponding temperature distribution along the CNT's axis. Note that all the images were taken without the presence of bias voltage.

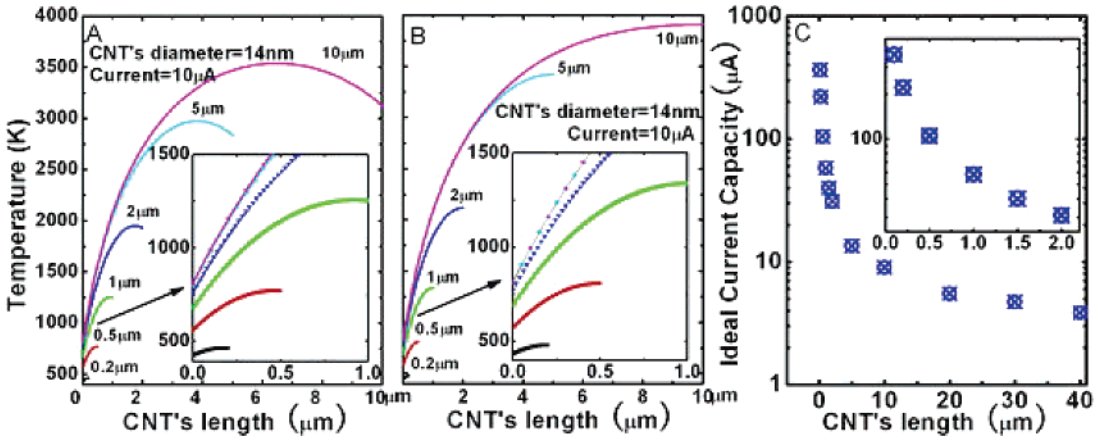

Figure 4. (A, B) The temperature distributions along the CNTs with various lengths at a fixed emission current 10 μA with (A) or without (B) considering the heat loss accompanying electron emission. (C) The calculated ideal emission current capacity for CNTs of various lengths by assuming no electrostatic force born on the CNTs during FE. The inset in (C) is a magnified picture of the first six plots.

Table 1. The Breaking Point for Four Samples of Ours and Doytcheva's

	1	2	3	Doy-1
length of CNT (nm)	470	330	1000	1000
diameter of CNT (nm)	14	14	10	21
exptl breaking point (nm)	390	280	880	900
theoretical T-max point (nm)	394.8	283.8	878.8	899.7

segment by segment breakdown, we must apply a very large current density, as well as a very high local E-field according to the F−N equation. Consequently in short CNT there will be a very high axial stress under which the contact between the CNT and microtip usually yields, leading to the runaway of short CNT emitter. Similar phenomena were also observed in Doytcheva et al.'s experiment.[13]

From the above discussion, failure and degradation of the field emitting CNT can be ascribed to two effects, the F-effect and the T-effect. Since CNTs have very strong covalent bonds, assuming a 11 GPa tensile stress as measured by Yu et al.,[20] a local E-field of 5 V/Å is required to initiate the field evaporation process. Due to the moderate work function of CNTs (4.6 eV),[21] a local E-field around 1 V/Å is sufficient to induce current heating. It is hard, therefore, to see the F-effect independently except that the CNT has severe mechanical defects or a weak contact with the microtip and was broken or torn away by the electrostatic force in low current. Similarly, it is also hard to see the absolute T-effect independent of the F-effect because of the high local E-field at the emitters during FE. Therefore, the failures or degradations observed are mostly induced by a combination of the F-effect and the T-effect. However, if there were severe defects in the CNT or weak contacts with microtip, the failures of the CNT usually take place at these weak points, which is mainly due to the F-effect. For high-quality CNT emitters with uniform diameters, the failures or degradations tend to occur in a segment by segment breakdown mode due to a combination of the F-effect and the T-effect. From Figure 4A, it is clear that the longer CNT will have a high

temperature at a smaller emission current. That is, longer CNTs have smaller current capacities as shown in Figure 4C (see Supporting Information[16]) and consequently will tend to fail at a small current density as well as a small E-field, where the T-effect is more prominent. Short CNT emitters with large current capacities (Figure 4C), when working at high current density, will experience a large E-field and consequently a large axial stress which are unfavorable to the emitter's stability. To further improve the stability of CNT emitters working at high current, we could modify the CNT's tip with well-chosen low work function materials such as Ti, Zr,[7] and the best LaB_6.[22]

In summary, we have improved the models of Vincent et al.[8] and Huang et al.[9] by considering the cooling effect accompanying field electron emission. This model predicts a maximum temperature occurring at an interior point rather than the tip of CNT during FE. When the contact between CNT and microtip is sufficiently strong, the failure of the CNT emitter tends to take place at the T-max point, leading to a segment by segment breakdown mode which is in good agreement with in situ TEM observations by Doytcheva et al.[13] and us. For practical applications, to fabricate stable CNT emitters with high current capacity, we should (1) use short high-quality CNTs, (2) ensure a good mechanical and electrical contact between CNT and microtip, and (3) modify the CNT's tip with low work function materials.

Finally, our model is one-dimensional based on the assumption that the CNT is open-ended with uniform diameter. Experimental observations indicate that, for close-ended CNTs, usually the complex tip structures were first destroyed by the T-effect and F-effect forming open-ended CNTs to which our model can be further applied.[23,24] Our model can also be applied to close-ended CNTs with stable tip structure, as long as the diameter of the CNT is uniform.

Acknowledgment. W. Wei, Y. Liu, and Y. Wei contributed equally to this work. We thank Abigail Curtis for proofreading and gratefully acknowledge the financial support from National Basic Research Program of China (2005CB623606) and NSFC (10334060,10434010)).

Supporting Information Available: The experimental details of sample preparation, the measurement of the sample resistivity and two probe configuration, and corresponding calculations for electrostatic force and ideal current capacity. This material is available free of charge via the Internet at http://pubs.acs.org.

References

(1) Yamamoto, S. *Rep. Prog. Phys.* **2006**, *69*, 181−232.
(2) Wang, Q. H.; Yan, M.; Chang, R. P. H. *Appl. Phys. Lett.* **2001**, *78*, 1294−1296.
(3) de Jonge, N.; Lamy, Y.; Schoots, K.; Oosterkamp, T. H. *Nature* **2002**, *420*, 393−395.
(4) de Jonge, N.; et al. *Phys. Rev. Lett.* **2005**, *94*, 186807.
(5) Cheng, Y.; et al. *Rev. Sci. Instrum.* **2004**, *75*, 3264−3267.
(6) Purcell, S. T.; Vincent, P.; Journet, C.; Binh, V. T. *Phys. Rev. Lett.* **2002**, *88*, 105502.
(7) Wei, W.; et al. *Nanotechnology* **2006**, *17*, 1994−1998.
(8) Vincent, P.; Purcell, S. T.; Journet, C.; Binh, V. T. *Phys. Rev. B* **2002**, *66*, 075406.
(9) Huang, N. Y.; et al. *Phys. Rev. Lett.* **2004**, *93*, 075501.
(10) Wang, Z. L.; Gao, R. P.; de Heer, W. A.; Poncharal, P. *Appl. Phys. Lett.* **2002**, *80*, 856−858.
(11) Bonard, J. M.; Klinke, C.; Dean, K. A.; Coll, B. F. *Phys. Rev. B* **2003**, *67*, 115406.
(12) Rinzler, A. G.; et al. *Science* **1995**, *269*, 1550−1553.
(13) Doytcheva, M.; Kaiser, M.; de Jonge, N. *Nanotechnology* **2006**, *17*, 3226−3233.
(14) Richardson, O. W. *Philos. Trans. R. Soc.* **1903**, *201*, 497.
(15) Herring, C.; Nichols, M. H. *Rev. Mod. Phys.* **1949**, *21*, 185−270.
(16) See Supporting Information.
(17) Collins, P. G.; Avouris, P. *Appl. Phys. A*: *Mater. Sci. Process.* **2002**, *74*, 329−332.
(18) Huang, J. Y.; et al. *Phys. Rev. Lett.* **2005**, *94*, 236802.
(19) Wang, M. S.; Wang, J.; Chen, Q.; Peng, L.−M. *Adv. Funct. Mater.* **2005**, *15*, 1825−1831.
(20) Yu, M. F.; et al. *Science* **2000**, *287*, 637−640.
(21) Liu, P.; et al. *Phys. Rev. B* **2006**, *73*, 235412.
(22) Wei, W.; et al. *Appl. Phys. Lett.*, in press.
(23) Wang, M. S.; Wang, J. Y.; Peng, L.-M. *Appl. Phys. Lett.* **2006**, *88*, 243108.
(24) Wang, M. S.; et al. *J. Phys. Chem. B* **2006**, *110*, 9397−9402.

NL061982U